

A Variational Approach for Volume-to-Slice Registration

No Author Given

No Institute Given

Abstract. In this work we present a new variational approach for image registration where part of the data is only known on a low-dimensional manifold.

Our work is motivated by navigated liver surgery. Therefore, we need to register 3D volumetric CT data and tracked 2D ultrasound (US) slices. The particular problem is that the set of all US slices does not assemble a full 3D domain. Other approaches use so-called compounding techniques to interpolate a 3D volume from the scattered slices. Instead of inventing new data by interpolation here we only use the given data.

Our variational formulation of the problem is based on a standard approach. We minimize a joint functional made up from a distance term and a regularizer with respect to a 3D spatial deformation field. In contrast to existing methods we evaluate the distance of the images only on the two-dimensional manifold where the data is known. A crucial point here is regularization. To avoid kinks and to achieve a smooth deformation it turns out that at least second order regularization is needed.

Our numerical method is based on Newton-type optimization. We present a detailed discretization and give some examples demonstrating the influence of regularization. Finally we show results for clinical data.

1 Introduction

In this paper we describe a new method for the registration of volumetric images to data that is given only on a low dimensional submanifold. The work is motivated by a clinical problem on improved resection of tissue by pre-operative intervention planning in liver surgery [1, 2]. Before an intervention an extensive planning including the definition of surgical paths and risk analysis is made. The planning is based on abdominal CT scans of the patient and subsequent segmentation of liver, liver segments, and vessels, cf. Figure 1(a). During the intervention the surgeon is guided by tracked ultrasound (US) images of the liver. Consequently, the pre-operative CT planning data has to be aligned to the actual deformation of the liver given by the US data.

A challenge in laparoscopic liver surgery is that the US data is recorded as a sequence of two dimensional slices in 3-space. Although the spatial ordering of the slices follows the scan path, they are not aligned and in general each slice can have an arbitrary position, cf. 1(b).

One approach for the registration of a CT volume and US slices is to use so-called compounding techniques. Therefore, in a first step the US slice data is compounded into volume by interpolation and subsequently standard volumetric image registration is applied. However, using compounding has several drawbacks [3–5]. and practical experiments showed that using this approach for registration performs poorly and did not produce reasonable results. Besides poor performance, matching volumetric CT data to artificially generated volumetric US data does not provide confidence in registration results for the surgeon.

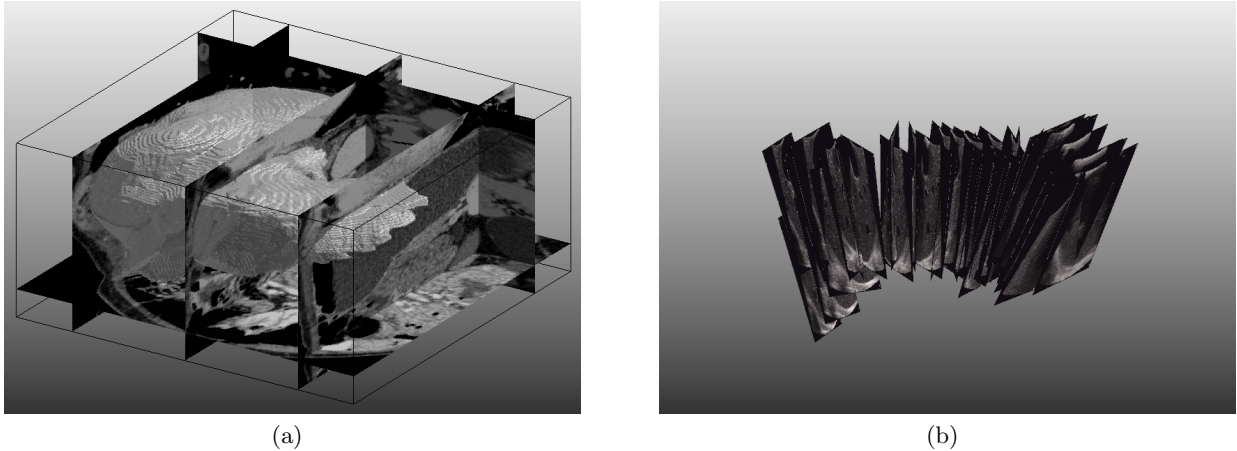


Fig. 1. Clinical image data; (a) pre-operative CT planning data (few slices out of volume and segmentation of the liver); (b) few US slices from a single scan.

Here, we take a different approach by comparing volumetric data directly to the given slice data. We use a variational setting for image registration. Therefore we minimize a cost-functional consisting of a so-called distance measure and regularizer with respect to a volumetric deformation. Here the regularizer is an integral on a d -dimensional domain while the distance is an integral on a $d-1$ -dimensional manifold. Although this seems to be a slight modification it turns out that higher order regularization is necessary to ensure smooth and differentiable deformations.

In this work we provide proof-of-concept for our new approach. Therefore we consider a simplified mono-modal setting, i.e., we assume the volumetric and the slice data stem from the same type of imaging device. Without loss of generality, this allows for using the easy to present so-called Sum-of-Squared distance measure for the description of our method.

The paper is organized as follows. First we present our variational approach to image registration and the novel distance measure. Next we discuss the need of higher-order regularization. In Section 4 we present a numerical scheme and subsequent we discuss our specific discretization of the distance measure and the regularizer in detail. Finally, in Section 5 we demonstrate the method with a synthesized clinical example.

2 Approach

In general we are given two images, a so-called reference $R : \mathbb{R}^d \rightarrow \mathbb{R}$ and a so-called template $T : \mathbb{R}^d \rightarrow \mathbb{R}$. The goal of image registration is to find a smooth deformation $y : \Omega \rightarrow \mathbb{R}^d$ that spatially aligns the images best on a domain of interest $\Omega \subset \mathbb{R}^d$. Typically Ω is a rectangular domain. Mathematically we formulate image registration as an optimization problem [6]. That is, we want to compute a solution y to

$$\min_y \mathcal{J}(y) := \mathcal{D}(R, T(y)) + \alpha \mathcal{S}(y) \quad (1)$$

where $T(y)$ denotes the composition $T \circ y$. The first term \mathcal{D} of the objective function is a so-called distance measure that quantifies similarity between the reference R and the deformed template $T(y)$. The second building block \mathcal{S} is a regularizer forcing smoothness of the solution where $\alpha > 0$ is a fixed chosen parameter. Typically \mathcal{S} has the form [7]

$$\mathcal{S}(y) := \frac{1}{2} \|\mathcal{B}y\|_{L_2(\Omega)}^2 \quad (2)$$

where \mathcal{B} is a linear differential operator.

The particular difficulty in our case is that the template is a volumetric image while the reference is only known on a few scattered slices. As mentioned in the introduction one can use compounding-techniques to generate an artificial volume and subsequently use standard distance measure that relies on comparing two images of same dimension.

We propose a different method. The idea of our new approach is to use only the given data rather than guessing the missing parts of the reference. To make the idea clear, in the following we assume that the distance measure is the so-called sum-of-squared-differences (SSD) [8], i.e. \mathcal{D} is the squared L_2 norm of the difference of the images. This is no loss of generality. The proposed modification applies to other distance measures such as mutual information [9, 10], too, which is more suitable for multi-modal registration of CT and US data. As mentioned in the introduction, the goal of this paper is proof-of-concept and to outline the general method. Therefore and for ease of presentation, here we use the SSD distance measure. However, the standard SSD for d -dimensional images is given by

$$\text{SSD}(R, T) = \frac{1}{2} \int_{\Omega} \left(T(x) - R(x) \right)^2 dx. \quad (3)$$

In our approach we assume the reference is given only on a few planes on Ω . More generally, we assume R is known only on a set of smooth and bounded $(d-1)$ -dimensional sub-manifolds $\mathcal{M}_j \subset \Omega$, $j = 1, \dots, m$. Therefore, we modify (3) and define our distance measure by

$$\mathcal{D}(R, T) := \frac{1}{2} \sum_{j=1}^m \int_{\mathcal{M}_j} \left(T(x) - R(x) \right)^2 dS(x) \quad (4)$$

where dS is the $(d-1)$ -dimensional surface measure. Note that in the particular case when \mathcal{M}_j are slices we can trace back our modified distance to a sum of SSD distances of $(d-1)$ -dimensional images similar to serial registration. In this particular case we can parametrize \mathcal{M}_j by linear maps τ_j with Gram determinant $\det D\tau_j^{\top} D\tau_j = 1$, where $D\tau_j$ denotes the Jacobian matrix of τ_j , such that

$$\mathcal{D}(R, T) = \sum_{j=1}^m \text{SSD}(R_j, T_j)$$

with $R_j := R \circ \tau_j$ and $T_j := T \circ \tau_j$.

Although changing integration in the distance measure seems a slight modification of problem (1) it turns out that regularization becomes crucial and needs to be chosen carefully. Since now the data is only given on a low-dimensional manifold the solution is strongly

influenced by the full-space regularization. It turns out that first-order regularization, e.g. by choosing $\mathcal{B} = \nabla$ in (2), will produce non-differentiable solutions with kinks at the boundary of the manifold, cf. Figure 2(e) and (h). In contrast, using second order regularization, e.g., setting $\mathcal{B} = \Delta$ where Δ denotes the vector Laplacian, produces smooth results, cf. Figure 2(f) and (i). In Section 3 we analyze this behavior by considering a simplified quadratic functional. Generally, the order of regularization to ensure differentiability depends on the space dimension. However, from the analysis in Section 3 we found that second order regularization is sufficient for space dimension $d = 2$ and $d = 3$. As a result we particularly propose using the curvature regularizer, i.e., setting $\mathcal{B} = \Delta$.

Summarizing, for volume-to-slice registration we consider problem (1) with the distance measure (4) and smoother (2) with $\mathcal{B} = \Delta$. Thus, our approach is

$$\min_y \frac{1}{2} \sum_{j=1}^m \int_{\mathcal{M}_j} \left(T(y(x)) - R(x) \right)^2 dS(x) + \frac{\alpha}{2} \int_{\Omega} |\Delta y|^2 dx. \quad (5)$$

3 Regularization

In the following we motivate second order so-called curvature regularization [11, 12] by choosing $\mathcal{B} = \Delta$. The resulting functional for the registration (cf. (5)) is highly non-linear and in general non-convex which makes an analysis difficult and involved. To illustrate the main point on regularization we now consider a simplified quadratic problem

$$\min_y \frac{1}{2} \|\mathcal{B}y\|_{L_2(\Omega)}^2 + \int_{\mathcal{M}} gy dS \quad (6)$$

where $\Omega \subset \mathbb{R}^d$ is a domain with smooth boundary (Lipschitz), $\mathcal{M} \subset \Omega$ is a smooth $(d-1)$ -dimensional manifold, and a function $g \in L_2(\mathcal{M})$. Without loss of generality we assume that locally coordinates can be chosen such that $\mathcal{M} = \{x \in \Omega : x_d = 0\}$. Then we can define a distribution f as the product of g multiplied by a Dirac-delta distribution, i.e., f is given by $f = g \delta_{x_d}$, such that

$$\int_{\Omega} fy dx = \int_{\Omega} g \delta_{x_d} y dx = \int_{\mathcal{M}} gy dS. \quad (7)$$

Furthermore we assume that $g \neq 0$, i.e., $\|g\|_{L_2(\mathcal{M})} \neq 0$. Computing the Euler-Lagrange equations in its weak form shows a necessary condition for a minimizer is

$$\mathcal{A}y = f \quad (8)$$

where $\mathcal{A} := -\mathcal{B}^* \mathcal{B}$ and \mathcal{B}^* denotes the adjoint of \mathcal{B} .

The right-hand-side f belongs to the space $H^{-1}(\Omega)$ but clearly $f \notin L_2(\Omega) = H^0(\Omega)$ where $H^{-1}(\Omega)$ denotes the dual space of $H^1(\Omega)$ and $H^m(\Omega)$ is the Sobolev space of all m -times weakly differentiable functions [13, §3].

Now we discuss two different choices for the regularizer \mathcal{B} . First first-order so-called diffusive regularization [14] with $\mathcal{B} = \nabla$ and second second-order curvature regularization by $\mathcal{B} = \Delta$.

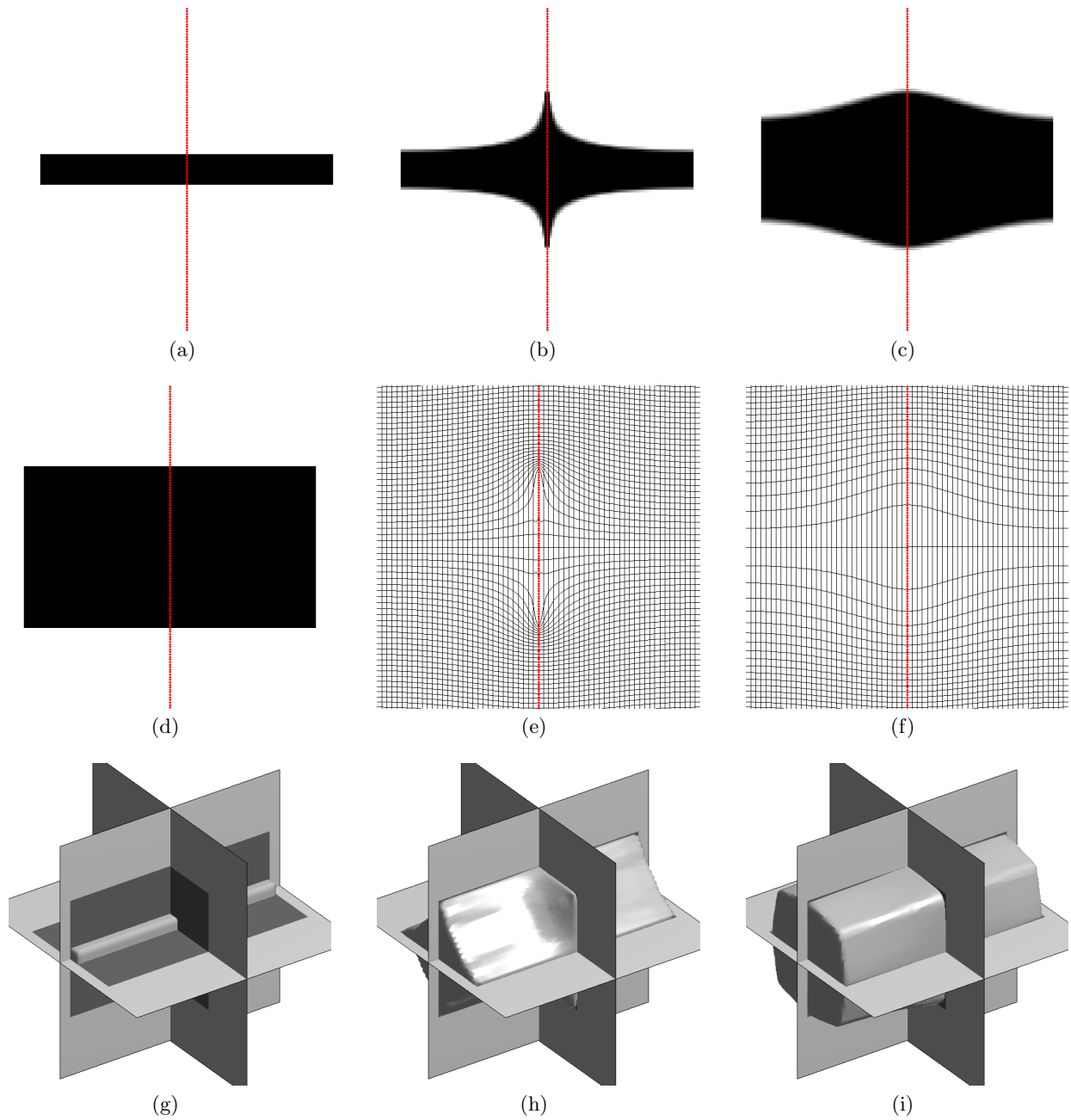


Fig. 2. Volume-to-slice-registration results for academic 2D (a)–(f) and 3D (g)–(i) experiments. (a) Template image and 1D manifold (vertical line); (d) Original Reference that is compared to the template on the 1D manifold (vertical line); (b)+(e) Deformed template (a) and deformation for 1st order regularization ($\mathcal{B} = \nabla$); (c)+(f) Deformed template (a) and deformation for 2nd order regularization ($\mathcal{B} = \Delta$); (g) Surface of 3D template (elongated bar) and three orthogonal 2D manifolds with reference data taken from a big cuboid; (h) Deformed template for 1st order regularization ($\mathcal{B} = \nabla$); (i) Deformed template for 2nd order regularization ($\mathcal{B} = \Delta$)

In the first case $\mathcal{B} = \nabla$ yields $\mathcal{B}^* = -\nabla \cdot$ and hence $\mathcal{A} = \Delta$ is a second-order differential operator. Since the right-hand-side f belongs to $H^{-1}(\Omega) \setminus H^0(\Omega)$ a solution of (8) must be in $H^{-1+2}(\Omega) \setminus H^{0+2}(\Omega) = H^1(\Omega) \setminus H^2(\Omega)$ (cf. [15, §8]). Due to the embedding $H^k(\Omega) \subset C^m(\Omega)$ for $m < k - d/2$ this shows that if $d > 1$ a solution cannot be differentiable [13, §6].

Applying the same logic in the second case for $\mathcal{B} = \Delta$, we find $\mathcal{B}^* = -\Delta$ yielding the fourth-order differential operator $\mathcal{A} = \Delta^2$. Therefore, a weak solution y of (8) has to satisfy $y \in H^3(\Omega) \setminus H^4(\Omega)$. Hence, if $d < 4$ then $y \in C^1(\Omega)$ such that a solution is continuously differentiable for $d = 2, 3$.

4 Numerical Method

In this section we describe our approach to compute a numerical solution for the volume-to-slice registration problem (5). Here, we follow the first-discretize-then-optimize paradigm. Therefore, we discretize the functional and subsequently apply Gauss-Newton optimization. We start by explaining our discretization.

In the following we particularly describe the discretization for the three-dimensional case, i.e., $d = 3$. That is, the domain of interest Ω is a subset of \mathbb{R}^3 and \mathcal{M}_j are two-dimensional manifolds. We assume that the domain of interest is rectangular, i.e.,

$$\Omega = (a_1, b_1) \times (a_2, b_2) \times (a_3, b_3) \quad \text{with } -\infty < a_i < b_i < \infty, \quad i = 1, 2, 3,$$

and \mathcal{M}_j are rectangular slices. For simplicity we assume that all slices \mathcal{M}_j are parametrized over the same parameter space Θ such that

$$\mathcal{M}_j = \{x = \tau_j(t) : t \in \Theta\} \quad \text{and} \quad \Theta := (0, \theta_1) \times (0, \theta_2)$$

with parametrizations $\tau_j : \Theta \subset \mathbb{R}^2 \rightarrow \mathcal{M}_j \subset \mathbb{R}^3$ given by

$$\tau_j(t) := Q_j t + b_j, \quad Q_j \in \mathbb{R}^{3 \times 2} \text{ such that } Q_j^\top Q_j = I \text{ and } b_j \in \mathbb{R}^3. \quad (9)$$

Note that the condition $Q_j^\top Q_j = I$ implies $\det D\tau_j^\top D\tau_j = 1$ where $D\tau_j$ denotes the Jacobian matrix of τ_j . This property simplifies computing the integrals on the manifolds and will be used later. We start with the discretization of the deformation and the distance measure. Subsequently we describe the discretization of the regularizer.

Discretization of the Deformation

We use a nodal discretization for the deformation y on Ω . Therefore, we introduce a uniform grid composed of $n_1 \times n_2 \times n_3$ cells with grid-spacing $h = (\frac{b_1-a_1}{n_1}, \frac{b_2-a_2}{n_2}, \frac{b_3-a_3}{n_3})$ and nodal grid points

$$\Omega^h := \left\{ x_k = x_0 + k \odot h : k \in \{0, \dots, n_1\} \times \{0, \dots, n_2\} \times \{0, \dots, n_3\} \right\}$$

where $x_0 = (a_1, a_2, a_3)$ and \odot denotes the Hadamard (point-wise) product of two vectors. Then, we collect the values $y(x_k) \in \mathbb{R}^3$ of the deformation at all $N = (n_1 + 1)(n_2 + 1)(n_3 + 1)$ nodal grid points $x_k \in \Omega^h$ in a grid-function, i.e., a vector $y^h \in \mathbb{R}^{3N}$.

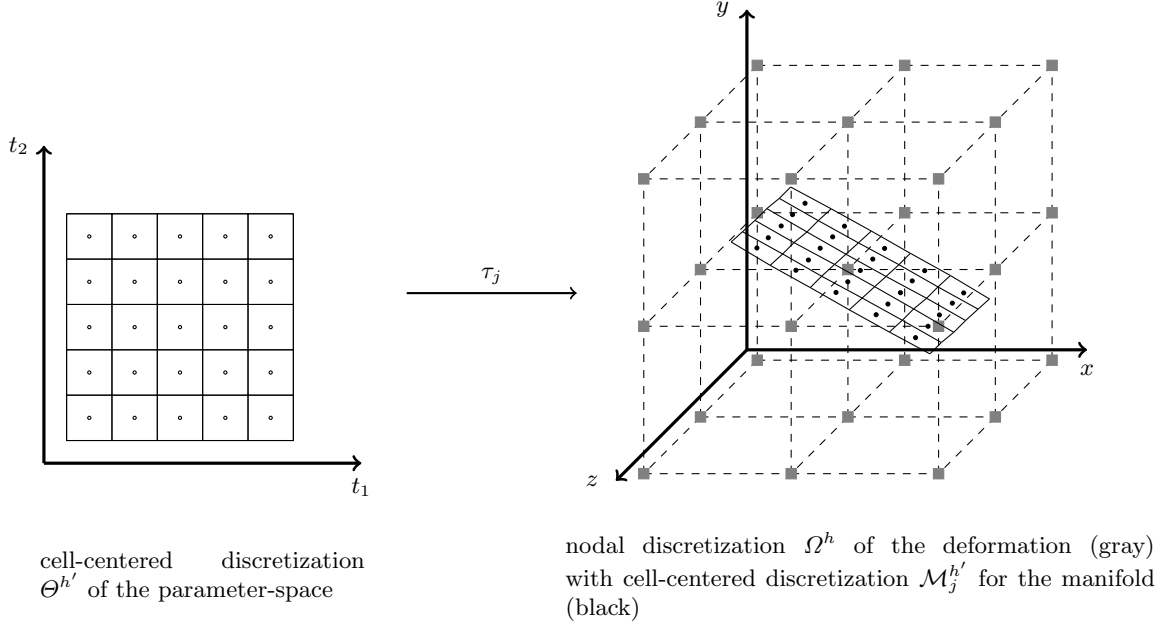


Fig. 3. Schematic overview on the discretization of the parameter-space Θ (left) and a manifold \mathcal{M}_j and the domain Ω (right).

Discretization of the Distance Measure

Now we turn to the discretization of the distance measure. Recall, that it was defined as

$$\mathcal{D}(R, T(y)) = \frac{1}{2} \sum_{j=1}^m \int_{\mathcal{M}_j} \left(T(y(x)) - R(x) \right)^2 dS(x).$$

For an approximation of the integrals on \mathcal{M}_j we start by discretizing the parameter space Θ . Therefore, we define

$$\Theta^{h'} := \left\{ t_k = k \odot h' - \frac{h'}{2} : k \in \{1, \dots, p_1\} \times \{1, \dots, p_2\} \right\} \quad \text{with} \quad h' = \begin{pmatrix} \theta_1 & \theta_2 \\ p_1 & p_2 \end{pmatrix}$$

such that $\Theta^{h'}$ contains the cell-center of a regular discretization by $p_1 \times p_2$ cells. Consequently, we discretize \mathcal{M}_j by

$$\mathcal{M}_j^{h'} := \{m_k = \tau_j(t_k) : t_k \in \Theta^{h'}\}.$$

Note that we have two different grid-spacings h and h' for the discretization of the deformation y on Ω and the discretization of the manifolds \mathcal{M}_j , respectively. An schematic overview of the different discretizations $\Theta^{h'}$, $\mathcal{M}_j^{h'}$, and Ω^h is shown in Figure 3. Using the common

mid-point rule for the discretization of an integral over \mathcal{M}_j we obtain

$$\begin{aligned}
\int_{\mathcal{M}_j} \left(T(y(x)) - R(x) \right)^2 dS(x) &= \int_{\Theta} \left(T(y(\tau_j(t))) - R(\tau_j(t)) \right)^2 \sqrt{\det D\tau_j^\top D\tau_j} dt \\
&= \int_{\Theta} \left(T(y(\tau_j(t))) - R(\tau_j(t)) \right)^2 dt \\
&\approx h'_1 h'_2 \sum_{t_k \in \Theta^{h'}} \left(T(y(\tau_j(t_k))) - R(\tau_j(t_k)) \right)^2 \\
&= h'_1 h'_2 \sum_{m_k \in \mathcal{M}_j^{h'}} \left(T(y(m_k)) - R(m_k) \right)^2,
\end{aligned}$$

where we used orthogonality of the Jacobian matrix $D\tau_j$, cf. (9). For short notation, analogues to the deformation we collect the $M = p_1 p_2$ grid points in $\mathcal{M}_j^{h'}$ in a vector $m_j^{h'} \in \mathbb{R}^{3M}$. With some abuse of notation let $R_j^{h'} := R(m_j^{h'}) \in \mathbb{R}^M$ be the values of the reference R on $\mathcal{M}_j^{h'}$ and analogues $T(y(m_j^{h'}))$ be the values of $T(y)$ such that

$$\|T(y(m_j^{h'})) - R_j^{h'}\|_2^2 = \sum_{m_k \in \mathcal{M}_j^{h'}} \left(T(y(m_k)) - R(m_k) \right)^2.$$

As we can see this approximation involves values of the deformation y at points $m_k \in \mathcal{M}_j^{h'}$ which are in general no grid-points of our nodal discretization Ω^h . To this end we approximate the values $y(m_k)$ for $m_k \in \mathcal{M}_j^{h'}$ by interpolation of the nodal grid-function y^h , i.e.,

$$y(m_k) \approx \sum_{i=1}^{3N} \xi_i y_i^h \quad \text{for } m_k \in \mathcal{M}_j^{h'}.$$

We particularly use linear interpolation such that in fact only 8 coefficients per point are involved. Collecting all interpolation weights ξ_i for each point $m_k \in \mathcal{M}_j^{h'}$ in a $3M \times 3N$ matrix P_j we have

$$T(P_j y^h) \approx T(y(m_j^{h'})).$$

Summarizing, we approximate the distance measure by

$$\mathcal{D}(R, T(y)) = \frac{1}{2} \sum_{j=1}^m \int_{\mathcal{M}_j} \left(T(y(x)) - R(x) \right)^2 dS(x) \approx \frac{h'_1 h'_2}{2} \sum_{j=1}^m \|T(P_j y^h) - R_j^{h'}\|_2^2.$$

Setting $R^{h'} = (R_1^{h'}, \dots, R_m^{h'}) \in \mathbb{R}^{Mm}$, $P = \text{diag}(P_1, \dots, P_m) \in \mathbb{R}^{3Mm \times 3N}$ we obtain a concise formulation for a discrete version of $\mathcal{D}(R, T(y))$ given by

$$D(y^h) := \frac{h'_1 h'_2}{2} \|T(P y^h) - R^{h'}\|_2^2. \tag{10}$$

Discretization of the Regularizer

For a discrete version of the curvature regularizer we use standard finite differences for approximating derivatives and the mid-point rule for the approximation integrals. Recall the curvature regularizer was defined as

$$\mathcal{S}(y) = \frac{1}{2} \|\Delta y\|_{L_2(\Omega)}^2 = \frac{1}{2} \int_{\Omega} |\Delta y|^2 dx.$$

In a first step we approximate the Laplacian based on the standard second-order seven-point-formula, i.e., we define

$$\Delta^h y(x) := \sum_{\ell=1}^3 \frac{1}{h_{\ell}^2} \left(y(x - h_{\ell} e_{\ell}) - 2y(x) + y(x + h_{\ell} e_{\ell}) \right)$$

where e_1, e_2, e_3 are the unit vectors of \mathbb{R}^3 . Furthermore, let $B^h \in \mathbb{R}^{3N \times 3N}$ be its matrix representation such that $B^h y^h$ is a second order approximation to Δy at the nodal grid points in Ω^h yielding $(B^h y^h) \odot (B^h y^h)$ is a second order approximation to $(\Delta y)^2$. Now, let $A_n^c \in \mathbb{R}^{n_1 n_2 n_3 \times N}$ be a matrix that averages values from nodes to the cell-centers such that $A_n^c (B^h y^h) \odot (B^h y^h)$ is a second order approximation to $(\Delta y)^2$ at the cell-centers. Thus applying the mid-point rule for mesh size $h = (h_1, h_2, h_3)$ we obtain

$$h_1 h_2 h_3 e^{\top} A_n^c (B^h y^h) \odot (B^h y^h) \approx \int_{\Omega} |\Delta y|^2 dx$$

with $e = (1, 1, \dots, 1) \in \mathbb{R}^{n_1 n_2 n_3}$ the one-vector. Moreover, applying some linear algebra we find

$$e^{\top} A_n^c (B^h y^h) \odot (B^h y^h) = e^{\top} A_n^c \text{diag}(B^h y^h) B^h y^h = y^{h\top} B^{h\top} \text{diag}(e^{\top} A_n^c) B^h y^h.$$

As a result, we define the discrete version of the curvature regularizer by

$$S(y^h) := \frac{1}{2} y^{h\top} A^h y^h$$

with a matrix $A^h := h_1 h_2 h_3 B^{h\top} \text{diag}(e^{\top} A_n^c) B^h \in \mathbb{R}^{3N \times 3N}$.

Gauss-Newton Optimization

Having established discrete versions of the distance measure and the smoother now we aim to

$$\min_y D(y^h) + \alpha S(y^h). \quad (11)$$

Clearly, (11) is not a quadratic function due to the non-linearity in the distance D . Therefore, we cannot compute a solution directly and have to rely on an iterative method. Here, we us

a standard Gauss-Newton method [16]. Therefore, in each iteration we solve a linear system of the type

$$Hs = -g \tag{12}$$

to compute an update s for the current iterate. Thereby g is the gradient $\nabla D + \alpha \nabla S$ of the objective function given by

$$g = h'_1 h'_2 P^\top \nabla T^\top (T(Py^h) - R^{h'}) + \alpha A^h y^h$$

and H is an approximation to the Hessian $\nabla^2 D + \alpha \nabla^2 S$. Neglecting second order terms in $\nabla^2 D$ we set

$$H := h'_1 h'_2 P^\top \nabla T^\top \nabla T P + \alpha A^h.$$

Thus, the Hessian is a sparse symmetric positive definite matrix such that we can apply a conjugate gradient (CG) method for solving the linear system (12). In our implementation we use CG with symmetric Gauss-Seidel relaxation as a preconditioner. Summarizing this leads to an efficient numerical algorithm for computing a solution to the discrete volume-to-slice registration problem (11).

5 Experiments

We demonstrate our method by an academic example on real liver data. Therefore, we use $238 \times 155 \times 156$ US volumetric data captured by a 3D US-scanner. We simulate a typical ultrasound sweep by extracting few 2D slices from the volume. Figure 4(a) shows the setting for five slices where we visualize the volumetric data by a surface rendering of the contained vessels. This slice data is used as reference. Subsequently, we apply an artificial non-linear deformation to the volume that is used as a template. Figure 4(b) displays a surface rendering of the template with the reference slice data. Based on the five reference slices and the volumetric template then we performed a volume-to-slice registration.

Figure 4(c) and 4(d) shows the 3D template vessels before and after registration together with original vessels. Note that the original vessels served only to generate the reference slices and was not take into account during registration. As we can see we obtain an amazing and almost perfect alignment based on very few reference data (see Figure 4(d)).

6 Conclusions

We described a new method for registration of a d -dimensional template to $d - 1$ -dimensional reference data motivated by CT/US registration. A key observation is that high order regularization is required to avoid unwanted and non-differentiable deformations. Furthermore, we described an efficient algorithmic based on a Gauss-Newton optimization method.

In a first experiment we successfully demonstrated our method for the registration of artificially deformed data where we were able to almost recover the original deformation based only on very few reference data.

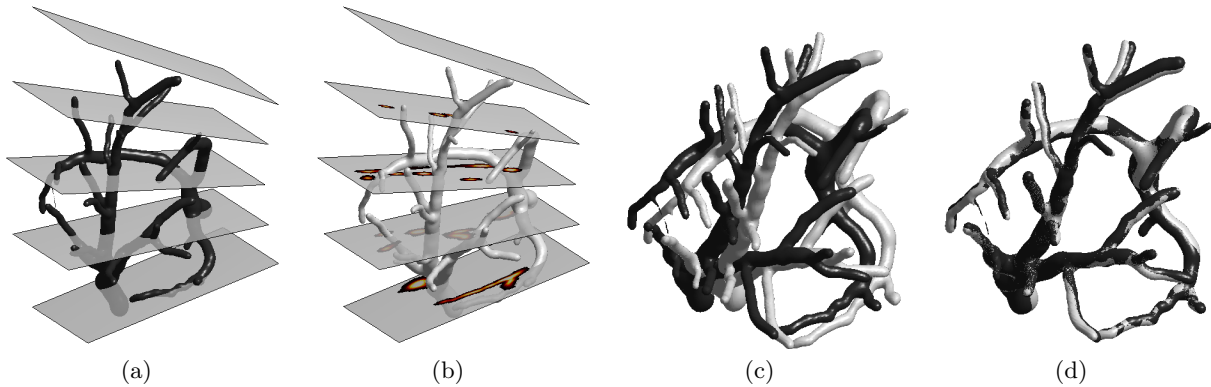


Fig. 4. 3D Volume-to-slice-registration results for clinical data. (a) 3D data (black) with five 2D reference slice; (b) 3D template (gray) with five reference slice; (c)+(d) 3D template (gray) and original data (black) before and after registration

These promising first result shows that our approach works in general. Clearly, the chosen SSD distance measure is not suitable for the target application on CT and US registration. However, our overall method is independent of a particular choice for the distance measure. An extension to other distance measure that can handle multi-modality, such as mutual information, is straightforward.

Concluding, we have presented a novel scheme and proof-of-concept for a clinical-relevant problem based on sound theory and efficient numeric. Future work includes extension to a multi-modal setting for registration of CT and US.

Acknowledgments

References

1. Fong, Y., Fortner, J., Sun, R., et al.: Clinical score for predicting recurrence after hepatic resection for metastatic colorectal cancer: analysis of 1001 consecutive cases. *Ann Surg* **230** (1999) 309–318
2. Lang, H.: Technik der leberresektion - teil i. *Chirurg* **78**(8) (2007) 761–774
3. Barry, C., Allott, C., John, N., Mellor, P., Arundel, P., Thomson, D., Waterton, J.: Three-dimensional freehand ultrasound: Image reconstruction and volume analysis. *Ultrasound in Medicine & Biology* **23** (1997) 1209–1224
4. Coupe, P., Azzabou, P.H.N., Barillot, C.: 3d freehand ultrasound reconstruction based on probe trajectory. In: *MICCAI Proceedings*. (2005) 597–604
5. Rohling, R.: 3D Freehand Ultrasound: Reconstruction and Spatial Compounding. PhD thesis, University of Cambridge, Department of Engineering (1998)
6. Broit, C.: Optimal registration of deformed images. PhD thesis, Department of Computer and Information Science, University of Pennsylvania (1981)
7. Modersitzki, J.: Numerical Methods for Image Registration. Numerical Mathematics and Scientific Computation. Oxford University Press (2003)
8. Brown, L.G.: A survey of image registration techniques. *ACM Computing Surveys* **24**(4) (1992) 325–376
9. Viola, P.A., Wells, W.M.I.: Alignment by maximization of mutual information. In: 5th International Conference on Computer Vision. (1995)
10. Collignon, A., Maes, F., Vandermeulen, P., Suetens, P., Marchal, G.: Automated multi-modality image registration based on information theory. *Information Processing in Medical Imaging* (1995)
11. Fischer, B., Modersitzki, J.: Curvature based image registration. *JMIV* **18**(1) (2003)
12. Fischer, B., Modersitzki, J.: Combining landmark and intensity driven registrations. *PAMM* **3** (2003) 32–35

13. Wloka, J.: Partial Differential Equations. Cambridge University Press (1987)
14. Fischer, B., Modersitzki, J.: Fast diffusion registration. In Nashed, M., Scherzer, O., eds.: Inverse Problems, Image Analysis, and Medical Imaging. Volume 313 of Contemporary Mathematics. AMS (2002)
15. Rudin, W.: Functional Analysis. McGraw-Hill (1991)
16. Nocedal, J., Wright, S.J.: Numerical Optimization. Springer Series in Operations Research. Springer (1999)